8.	4-chloronitrobenzene	−2.85	−1.83	−2.66	11
9.	2,5-PCB	−5.06	−5.75	−5.45	27
10.	2,6-PCB	−5.21	−5.52	−5.35	27
11.	2,4,6-PCB	−6.06	−6.24	−5.88	27
12.	fluorene	−4.92	−4.43	−4.78	10
13.	pyrene	−6.17	−6.04	−6.39	10
14.	indan	−3.04	−3.10	−3.27	10
15.	3-methylpyridine	0.04	−0.01	−0.17	11
16.	isoquinoline	−1.45	−1.11	−1.24	11
17.	tetrahydrofuran	0.48	0.59	0.74	11
18.	cortisone	−3.27	−2.95	−3.55	25
19.	2-naphthol	−2.25	−2.08	−1.61	25

[a] Estimation of log W using neural networks which gives a standard deviation 0.43. The standard deviation is 0.37 if we leave out the 4-chloronitrobenzene. [b] Estimation of log W using regression analysis which gives a standard deviation 0.36.

found to be superior to that obtained with the regression analysis approach, 0.30. The results clearly demonstrate that the neural network has captured the association between the selected properties of an organic compound and its aqueous solubility.

The trained neural network was tested on its ability to predict the aqueous solubility of an unknown set of organic compounds, that is, the compounds were not members of the original training set and indeed in some cases were quite unrelated to the original members. The test set should therefore provide a severe test of value predicted for 4-chloronitrobenzene is probably due to the omission from the training set of any chloronitro compound which would reduce the credence attached to the predicted value.

In conclusion, a neural network model has been applied to the prediction of the aqueous solubility of organic compounds and the usefulness of the model clearly demonstrated. The predictive capability of neural networks has been demonstrated on a number of unknown organic compounds. It has been shown in this study that neural networks give a superior performance to that given by a regression analysis technique. While this work was in progress a paper was published[34] describing an application of the neural network approach to estimating quantitative structure–activity relationships. This work confirms the conclusions derived in this study that neural networks can determine such relationships with a performance exceeding that of linear multiregression analysis. Clearly, the neural network approach would seem to have great potential for determining quantitative structure–activity relationships and as such be a valuable tool for the medicinal chemist.

Supplementary Material Available: Listing of complete experimental and estimated log W values (6 pages). Ordering information is given on any current masthead page.

(34) Aoyoma, T.; Suzuki, Y.; Ichikawa, H. *J. Med. Chem.* 1990, *33*, 2583.

Computational Studies on FK506: Conformational Search and Molecular Dynamics Simulation in Water

Julianto Pranata and William L. Jorgensen*

Contribution from the Department of Chemistry, Yale University, New Haven, Connecticut 06511.
Received May 6, 1991

Abstract: Computational investigations have been undertaken to elucidate the conformational characteristics and the hydration of the immunosuppresant FK506. The calculations made use of the AMBER/OPLS molecular mechanics force field, augmented with some newly developed parameters particularly for the α-ketoamide torsion. A conformational search on FK506 using an internal coordinate Monte Carlo method found 21 distinct energy minima within 12 kcal/mol of the lowest energy structure. The minima include structures with both cis and trans conformations of the amide bond. A 200-ps molecular dynamics simulation in water then provided information on the dynamical behavior of the cis isomer of FK506 as well as its hydration. Two conformations of the macrocyclic ring are sampled during the simulation, and some exocyclic groups undergo rapid conformational changes. Considerable flexibility is also observed near the amide functionality, which is in the binding region of FK506. The hydration of FK506 shows interesting variations owing to differences in the steric environments of potential hydrogen-bonding sites. In the critical binding region, there are on average 5 hydrogen bonds between water molecules and FK506.

FK506, rapamycin, and cyclosporin A (CsA) are immunosuppresive agents that act by blocking the signal transduction pathways that lead to T lymphocyte activation.[1] FK506 and rapamycin are structurally similar and appear to bind to the same receptor, FKBP,[2] while the structurally unrelated CsA, a cyclic undecapeptide, binds to a different receptor, cyclophilin.[3] Both receptors have been shown to be peptidyl-prolyl cis–trans isomerases (rotamases).[4,5] FK506 and rapamycin inhibit the rotamase activity of FKBP, but not of cyclophilin; likewise CsA inhibits the rotamase activity of cyclophilin, but not of FKBP.[4]

(1) Schreiber, S. L. *Science* 1991, *251*, 283.
(2) Bierer, B. E.; Mattila, P. S.; Standaert, R. F.; Herzenberg, L. A.; Burakoff, S. J.; Crabtree, G.; Schreiber, S. L. *Proc. Natl. Acad. Sci. U.S.A.* 1990, *87*, 9231. Dumont, F. J.; Melino, M. R.; Staruch, M. J.; Koprak, S. L.; Fischer, P. A.; Sigal, N. H. *J. Immunol.* 1990, *144*, 1418. Fretz, H.; Albers, M. W.; Galat, A.; Standaert, R. F.; Lane, W. S.; Burakoff, S. J.; Bierer, B. E.; Schreiber, S. L. *J. Am. Chem. Soc.* 1991, *113*, 1409.
(3) Handschumacher, R. E.; Harding, M. W.; Rice, J.; Drugge, R. J.; Speicher, D. W. *Science* 1984, *226*, 544. Handschumacher, R. E.; Harding, M. W. *Transplantation* 1988, *46*, 29S.
(4) Harding, M. W.; Galat, A.; Uehling, D. E.; Schreiber, S. L. *Nature* 1989, *341*, 758. Siekierka, J. J.; Hung, S. H. Y.; Poe, M.; Lin, C. S.; Sigal, N. H. *Nature* 1989, *341*, 755.
(5) Fischer, G.; Wittmann-Liebold, B.; Lang, K.; Kiefhaber, T.; Schmid, F. X. *Nature* 1989, *226*, 544. Takahashi, N.; Hayano, T.; Suzuki, M. *Nature* 1989, *226*, 473.

0002-7863/91/1513-9483$02.50/0

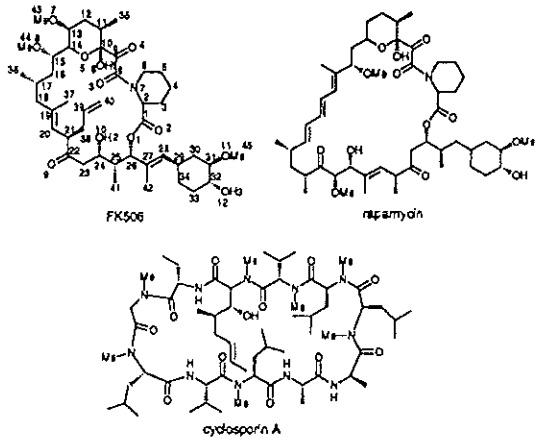

Crystal structures of all three immunosuppresants have been reported.[6-8] In addition, NMR data have been used to deduce the structure of CsA in a variety of solvents.[6,9] The solution-phase structure for FK506 in $CDCl_3$ has also been examined.[10]

Schreiber and co-workers have investigated the inhibition of FKBP rotamase activity by FK506.[11] The immunosuppresant with ^{13}C labels at C8 and C9 was synthesized[12] and used to probe the binding process. ^{13}C NMR of the enzyme–inhibitor complex shows no evidence for the existence of a tetrahedral adduct at either C8 or C9. Thus, the mechanism for rotamase activity does not involve the formation of a tetrahedral intermediate; rather, a mechanism was proposed which features a twisted amide bond in the transition state. The α-ketoamide functionality in FK506 (and rapamycin) has an orthogonal orientation in the crystal structure[7,8] and serves as a surrogate for the twisted amide bond. Thus, by acting as a transition-state analogue, FK506 potently inhibits rotamase activity.

Interestingly, the NMR of FK506 in solution shows the existence of two isomers, attributed to the cis and trans conformations for the amide bond in a 2:1 ratio.[10,11] It has recently been determined by X-ray crystallography that the trans isomer is bound to FKBP,[13] though only the cis isomer is observed in the crystal structure of isolated FK506.[7] For CsA, both in the crystal and in solution the molecule has a cis peptide bond between residues MeLeu 9 and MeLeu 10.[6,9] However, there is evidence that CsA bound to cyclophilin also adopts a trans conformation for this bond.[14]

On the computational side, Lautz et al. have reported molecular dynamics simulations of CsA in water, CCl_4, and the crystalline environment.[15] The focus was on comparisons with experimental structural data and medium effects on the conformation of CsA. However, the 40–50-ps durations for the simulations severely limited the conformational sampling.

We are interested in investigating the structural and energetic aspects of the binding of immunosuppresants and substrates to FKBP. The initial efforts, described here, addressed the development of needed force-field parameters for FK506, conformational search for low-energy structures in the absence of solvent, and characterization of the hydration and internal motions of FK506 through a 200-ps molecular dynamics simulation in water.

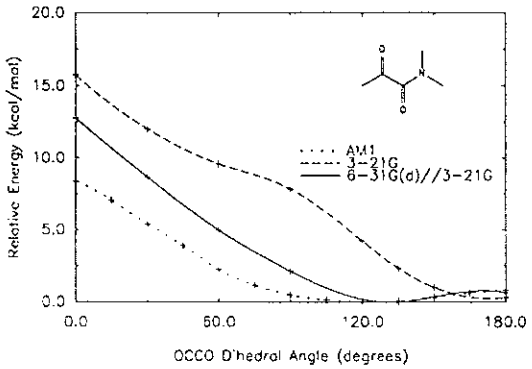

Figure 1. Torsional profiles of *N*,*N*-dimethyl-α-ketopropanamide from molecular orbital calculations.

Parameter Development

A principal difficulty in performing computations on molecules like FK506 is the lack of appropriate molecular mechanics parameters. For proteins and nucleic acids, a variety of standard parameter sets are available, e.g., AMBER[16] or CHARMm.[17] However, FK506 contains functionalities not found in peptides or nucleotides. In particular, an accurate description of the α-ketoamide torsion is required, in view of its importance in the binding process.[11]

Where available, parameters and potential functions from the AMBER force field were used for bonded interactions (bond stretches, bends, and torsions, including improper torsions).[16] The OPLS parameters and functions were used for nonbonded interactions.[18] Some parameters were added to the AMBER set on the basis of existing parameters for similar functional groups. Appropriate parameters were not found for some torsions involving esters, ketones, and olefins. Parameters appropriate for an ester group were recently developed by Charifson et al.[19] and were used in the present work. Other torsional parameters were obtained by fitting to ab initio torsional profiles calculated by Wiberg and co-workers.[20] A united-atom model has been here for CH_n units, otherwise all atoms are explicitly represented.

As mentioned above, the α-ketoamide torsion is particularly important, and the parameters for this functionality were developed with the aid of quantum mechanical calculations. *N*,*N*-Dimethyl-α-ketopropanamide was chosen as a model system, and the torsional profile for the bond between the two carbonyl carbons was computed using semiempirical (AM1)[21,22] and ab initio

(6) Loosli, H. R.; Kessler, H.; Oschkinat, H.; Weber, H. P.; Petcher, T. J.; Widmer, A. *Helv. Chim. Acta* **1985**, *68*, 682.
(7) Tanaka, H.; Kuroda, A.; Marusawa, H.; Hatanaka, H.; Kino, T.; Goto, T.; Hashimoto, M.; Taga, T. *J. Am. Chem. Soc.* **1987**, *109*, 5031. Taga, T.; Tanaka, H.; Goto, T.; Tada, S. *Acta Crystallogr.* **1987**, *C43*, 751.
(8) Swindells, D. C. N.; White, P. S.; Findlay, J. A. *Can. J. Chem.* **1978**, *56*, 2491.
(9) Kessler, H.; Oschkinat, H.; Loosli, H. R. *Helv. Chim. Acta* **1985**, *68*, 661. Kessler, H.; Köck, M.; Wein, T.; Gehrke, M. *Helv. Chim. Acta* **1990**, *73*, 1818.
(10) Karuso, P.; Kessler, H.; Mierke, D. F. *J. Am. Chem. Soc.* **1990**, *112*, 9434.
(11) Rosen, M. K.; Standaert, R. F.; Galat, A.; Nakatsuka, M.; Schreiber, S. L. *Science* **1990**, *248*, 863.
(12) Nakatsuka, M.; Ragan, J. A.; Sammakia, T.; Smith, D. B.; Uehling, D. E.; Schreiber, S. L. *J. Am. Chem. Soc.* **1990**, *112*, 5583.
(13) Van Duyne, G. D.; Standaert, R. F.; Karplus, P. A.; Schreiber, S. L.; Clardy, J. *Science* **1991**, *252*, 839.
(14) Fesik, S. W.; Gampe, R. T., Jr.; Holzman, T. F.; Egan, D. A.; Edalji, R.; Luly, J. R.; Simmer, R.; Helfrich, R.; Kishore, V.; Rich, D. H. *Science* **1990**, *250*, 1406.
(15) Lautz, J.; Kessler, H.; van Gunsteren, W. F.; Weber, H. P.; Wenger, R. M. *Biopolymers* **1990**, *29*, 1669. Lautz, J.; Kessler, A.; Kaptein, R.; van Gunsteren, W. F. *J. Computer-Aided Mol. Design* **1987**, *1*, 219.
(16) Weiner, S. J.; Kollman, P. A.; Case, D. A.; Singh, U. C.; Ghio, C.; Alagona, G.; Profeta, S., Jr.; Weiner, P. *J. Am. Chem. Soc.* **1984**, *106*, 765. Weiner, S. J.; Kollman, P. A.; Nguyen, D. T.; Case, D. A. *J. Comp. Chem.* **1986**, *7*, 230.
(17) Brooks, B. R.; Bruccoleri, R. E.; Olafson, B. D.; States, D. J.; Swaminathan, S.; Karplus, M. *J. Comp. Chem.* **1983**, *4*, 187. Nilsson, L.; Karplus, M. *J. Comp. Chem.* **1986**, *7*, 591.
(18) Jorgensen, W. L.; Tirado-Rives, J. *J. Am. Chem. Soc.* **1988**, *110*, 1657. Jorgensen, W. L.; Briggs, J. M.; Contreras, M. L. *J. Phys. Chem.* **1990**, *94*, 1683.
(19) Charifson, P. S.; Hiskey, R. G.; Pedersen, L. G. *J. Comp. Chem.* **1990**, *10*, 1181.
(20) Wiberg, K. B.; Martin, E. *J. Am. Chem. Soc.* **1985**, *107*, 5035. Wiberg, K. B. *J. Am. Chem. Soc.* **1986**, *108*, 5817. Wiberg, K. B.; Laidig, K. E. *J. Am. Chem. Soc.* **1987**, *109*, 5935.
(21) Dewar, M. J. S.; Zoebisch, E. G.; Healy, E. F.; Stewart, J. J. P. *J. Am. Chem. Soc.* **1985**, *107*, 3902.
(22) AM1 calculations were performed using the MOPAC program. Stewart, J. J. P. MOPAC 5.0; QCPE Program No. 455; Indiana University, Bloomington, IN.

Table I. New AMBER Torsion Parameters

torsion	$V_1/2$	γ	$V_2/2$	γ	$V_3/2$	γ
			Ester			
CH—C(=O)—O—C[a]	2.545	0.0				
O=C—O—C[a]			4.150	180.0		
O—C(=O)—CH—X	0.470	0.0	0.500	180.0		
			Ketone			
C—C(=O)—C—X	0.203	0.0	0.230	180.0		
C—C(=O)—CH—X	0.305	0.0	0.345	180.0		
C—C(=O)—CH_2—X	0.610	0.0	0.690	180.0		
			Olefin			
X—C=C—X			7.500	180.0		
C=CH—CH_2—X	0.700	180.0			1.100	180.0
C=CH—CH—X	0.350	180.0			0.550	180.0
C=C—CH_2—X	0.350	180.0			0.550	180.0
C=C—CH—X	0.175	180.0			0.275	180.0
C—C(=C)—CH_2—X	0.350	0.0			0.550	0.0
C—C(=C)—CH—X	0.175	0.0			0.275	0.0
			α-Ketoamide			
O=C—C=O	0.12	180.0	0.42	180.0		
O=C—C—N	0.12	0.0	0.42	180.0		
C—C—C=O	0.12	0.0	0.42	180.0		
C—C—C—N	0.12	180.0	0.42	180.0		

[a] Reference 19.

(HF/3-21G and HF/6-31G(d)//3-21G)[23,24] molecular orbital calculations. The results are shown in Figure 1. Both the AM1 and 6-31G(d) calculations predict a nonplanar minimum, although the barrier at the anti conformation is quite low. For AM1, the minimum occurs at 124° and the height for the anti barrier is 0.79 kcal/mol, while the corresponding values from the 6-31G(d) calculations are 135° and 0.65 kcal/mol. However, the 3-21G results appear to overestimate the stability of the anti conformation, making it the minimum. In the crystal structures, the α-ketoamide functionality in both FK506 and rapamycin has an orthogonal orientation.[7,8] The same trend is observed in other molecules when this functionality is doubly substituted at the nitrogen; e.g., tetramethyloxamide is twisted by 71°.[25]

AMBER-type parameters were then obtained by fitting to the 6-31G(d) torsional profile. The fitting took into account the substantial nonbonded interactions in this molecule. In fact, it turned out that the nonbonded (i.e., steric) interactions are solely responsible for the nonplanarity of the system; there is nothing unusual about the torsional parameters that are reported in Table I.

As a test of the new parameters, they were incorporated into AMBER and used to compute the torsional profile of a non-macrocyclic fragment of the FK506 structure. This is compared to the profile computed using AM1 in Figure 2. Although the AMBER profile has a shallower minimum, the difference is not great, and the two profiles have the same overall shape. The minimum in the results with AMBER occurs at −108°, compared to −96° with AM1, while in the crystal structure of FK506 this torsional angle is −89°.[7]

All of the torsional parameters added to the AMBER set for the purpose of this work are presented in Table I. In addition, a complete listing of the parameters for FK506 is given in the Supplementary Material. The same parameters were used for the conformational search and molecular dynamics.

Conformation Search

Procedure. A fairly extensive search for the conformational minima of FK506 in the ideal gas phase was performed using an internal coordinate Monte Carlo method.[26] The focus was on the conformation of the 21-membered macrocycle. No search was conducted which involved variations of the exocyclic torsions. Also excluded were torsions within six-membered rings, namely those for the C2–N7, C10–O5, and O5–C14 bonds, as well as the double bond (C19–C20). The remaining 17 dihedral angles were randomly varied; however, O1–C1 was defined as the ring-closure bond, so its torsion and the torsions around the two adjacent bonds (C1–C2 and C26–O1) were not explicitly varied. Of course, no constraints were applied in the subsequent energy minimizations.

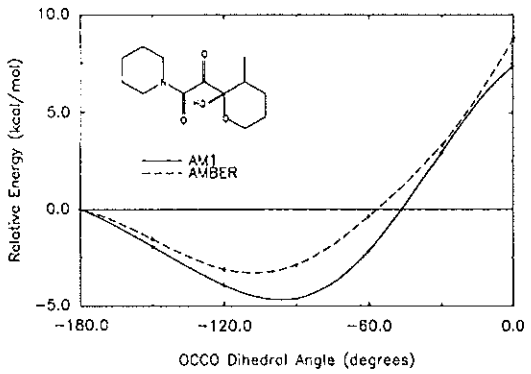

Figure 2. Torsional profiles of a fragment of FK506.

The starting structure for the search was obtained from the X-ray crystal structure.[7] Initially, all hydrogens bound to carbons were removed, resulting in representation of FK506 as 60 explicit atoms. This structure was energy minimized, and the resulting structure was used to start the conformational search. The RMS deviation between the actual X-ray structure and the energy-minimized form is only 0.48 Å. The only significant change is the formation of a hydrogen bond between O6–H1 and O4 that is not in the crystal structure (vide infra). A total of 8499 structures were generated using a random walk procedure; these were initially minimized to a root mean square gradient of 1 kJ/(mol·Å) (=0.239 kcal/(mol·Å)). Nonduplicate structures whose energies were within 50 kJ/mol (=12 kcal/mol) above the lowest energy minimum were saved. This resulted in 28 structures which were further minimized to a root mean square gradient of

(23) Hehre, W. J.; Radom, L.; Schleyer, P. v. R.; Pople, J. A. *Ab Initio Molecular Orbital Theory*; Wiley: New York, 1986.
(24) Ab initio calculations were performed using the GAUSSIAN 90 programs. Frisch, M. J.; Head-Gordon, M.; Trucks, G. W.; Foresman, J. B.; Schlegel, H. B.; Raghavachari, K.; Robb, M. A.; Binkley, J. S.; Gonzalez, C.; Defrees, D. J.; Fox, D. J.; Whiteside, R. A.; Seeger, R.; Melius, R.; Baker, J.; Martin, R. L.; Kahn, L. R.; Stewart, J. J. P.; Topiol, S.; Pople, J. A. GAUSSIAN 90 Revision F; Gaussian Inc.: Pittsburgh, PA, 1990.
(25) Adiwidjaja, G.; Voss, J. *Chem. Ber.* **1977**, *110*, 1159.
(26) Chang, G.; Guida, W. C.; Still, W. C. *J. Am. Chem. Soc.* **1989**, *111*, 4379.

Table II. Values of Macrocyclic Dihedral Angles (deg) in the Conformations Found in the Monte Carlo Search and in the X-ray Structure

	conformation								
dihedral angle	1	2	3	4	5	6	7	8	9
O1C1C2N7[b]	43	86	−168	179	87	91	−179	−178	−165
C1C2N7C8[c]	−95	−93	−100	−100	−101	−95	−100	−99	−100
C2N7C8C9	165	0	−2	0	−5	1	−3	2	−4
N7C8C9C10	167	−63	−105	−115	−96	−68	−99	−87	−104
C8C9C10O5	75	90	65	55	72	91	68	81	68
C9C10O5C14[c]	177	179	173	169	178	178	179	175	177
C10O5C14C15[c]	−177	−179	−176	−176	−177	−176	−177	−175	−177
O5C14C15C16	75	86	62	49	76	85	78	75	92
C14C15C16C17	57	65	65	52	68	68	60	89	−78
C15C16C17C18	−168	−172	−151	−159	−169	−170	−179	−170	−159
C16C17C18C19	60	66	−63	155	70	74	60	−56	167
C17C18C19C20	−107	−121	71	130	−123	−119	−126	16	−67
C18C19C20C21[c]	176	−179	175	175	−177	−176	−176	171	179
C19C20C21C22	−115	−123	−142	−115	−124	−110	−124	−118	−129
C20C21C22C23	73	106	83	101	122	−39	138	−48	101
C21C22C23C24	−152	−99	178	−120	148	122	−157	−148	174
C22C23C24C25	−58	−65	146	172	172	175	169	−64	169
C23C24C25C26	−71	−145	−61	−69	−84	−163	−69	−65	−67
C24C25C26O1	−40	−56	−23	−42	45	−55	−37	−24	−23
C25C26O1C1[b]	−154	−154	−147	−146	−147	−153	−149	−155	−147
C26O1C1C2[b]	−175	−169	−162	−177	−160	−169	−176	−171	−165
energy[d]	17.6	20.6	23.3	23.9	24.4	24.5	25.7	25.9	26.4

[a] After minimization. [b] O1C1 is defined as the ring closure bond, thus these dihedral angles are not explicitly included in the search. [c] These

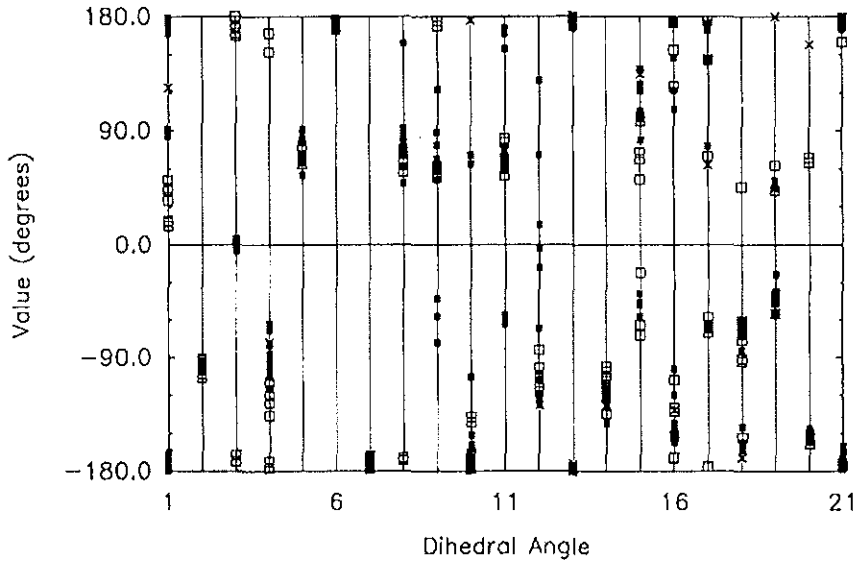

Figure 3. Distribution of macrocyclic dihedral angles in the 21 structures found in the Monte Carlo search. Open squares are for trans amide isomers and filled squares for cis. Also shown are the dihedral angles of the X-ray structure after minimization (×). The numbers of the dihedral angles on the abscissa correspond to the list in Table II.

0.1 kJ/(mol·Å). After elimination of duplicates and high-energy structures, 21 distinct minima were found.

The energy minimizations were performed using a dielectric constant of 1.0 and a cutoff distance of 9.0 Å for both van der Waals and electrostatic interactions. The calculations were performed with the BATCHMIN program, Version 2.7, on a DEC VaxStation 3500 minicomputer.[27]

Results. The dihedral angles for the macrocyclic ring in the 21 conformational minima found during the search are listed in Table II along with relative potential energies. A distribution of the dihedral angles is represented in Figure 3. Both Table II and Figure 3 also contain data for the conformation from the X-ray structure after minimization. The 21 energy minima include both trans and cis amide isomers. Stereopictures of the lowest energy trans (**1**) and cis (**2**) forms are shown in Figure 4, along with the energy minimized X-ray structure; corresponding pictures and coordinates for all 22 structures are available in the Supplementary Material.

It is emphasized that we did not attempt to locate *all* the conformational minima of FK506; to do so would have necessitated a much longer search as well as the inclusion of variations of the exocyclic and six-membered-ring torsions. However, the 21 structures may be expected to be representative of the low-energy conformations of FK506.

All 21 structures are reasonable in that no bonds or angles are unduly strained. Somewhat surprisingly, the X-ray crystal structure is not among these 21 structures. Its energy, or rather, the energy of the minimum closest to it, is 14.7 kcal/mol above the energy of the lowest minimum found. A minimization was

(27) BATCHMIN is the noninteractive part of the MACROMODEL molecular modeling program. Mohamadi, F.; Richards, N. G. J.; Guida, W. C.; Liskamp, R.; Lipton, M.; Caufield, C.; Chang, G.; Hendrickson, T.; Still, W. C. *J. Comp. Chem.* **1990**, *11*, 440.

conformation												
10	11	12	13	14	15	16	17	18	19	20	21	X-ray[a]
51	176	19	35	45	167	18	−172	173	19	89	15	124
−95	−98	−98	−106	−103	−97	−91	−99	−99	−92	−98	−94	−93
167	2	180	−172	−167	5	167	−2	−2	171	−3	167	0
152	−90	−172	−110	−120	−80	−136	−79	−115	−126	−88	−177	−78
78	72	69	75	69	84	67	89	72	64	81	69	87
175	172	174	170	173	175	172	176	176	170	177	173	176
−178	−170	−175	−168	−169	−177	−174	−169	−177	−173	−174	−177	−176
66	159	72	−169	−171	76	66	78	86	58	82	74	80
60	−43	57	177	173	79	60	123	−57	54	65	62	63
−170	−105	−166	−137	−141	−162	−178	64	71	−170	−177	−174	177
62	77	67	81	84	−57	63	72	171	55	65	68	63
−113	−127	−105	−98	−84	−3	−104	−108	−18	−113	−122	−117	−128
178	−175	−179	176	180	178	−177	180	177	174	−177	−179	−174
−118	−120	−106	−122	−97	−112	−101	−115	−122	−134	−117	−117	−122
68	139	−64	52	−72	−57	−22	−46	105	98	127	101	135
−169	−154	125	175	154	107	−133	−142	−142	−130	−147	−108	−132
−58	173	146	−70	70	78	−176	−68	173	177	172	−64	63
−68	−73	−76	−93	−153	−157	46	−63	−68	−61	−162	−91	−169
−40	−41	−45	−55	−55	−47	43	−23	−38	63	51	−45	180
−151	−149	−152	−151	−158	−154	69	−155	−150	65	−155	−155	158
−174	−178	179	178	177	−170	173	−167	177	160	−165	175	173
26.4	26.7	26.7	26.8	27.0	27.4	27.4	27.5	27.7	28.2	28.3	28.3	32.3

dihedral angles are not included in the search. [a] Energies in kcal/mol.

also carried out starting with the geometry of bound FK506 obtained from the X-ray crystal structure of its complex with FKBP.[13] The resultant structure had an energy 21.5 kcal/mol above the lowest energy minimum.

Interestingly, the cis isomers appear to favor a perpendicular orientation of the adjacent carbonyl groups (C8–C9 dihedral angle), while the trans isomers are more tolerant of an anti orientation in this position. Another noticeable difference is that the conformation about the C1–C2 bond is always gauche-like in the trans isomers; it is usually anti in the cis. These trends, of course, only reflect the results for the 21 structures. However, these torsions are in the binding region of FK506, and the tendencies they show may be important in view of the observation that only the trans isomer is bound to FKBP.[13] No other trends are strikingly apparent which differentiate the cis and trans isomers.

Not surprisingly, the four torsions excluded from the search (those around the C2–N7, C10–O5, O5–C14, and C19–C20 bonds) remain in their initial conformation (Figure 3). Three other torsions also show no tendency for variations, namely those around the C9–C10, C20–C21, and O1–C1 bonds. The anti orientation for the last torsion means that the ester is always in the *Z* form. Most of the rest of the torsions are clustered into easily identifiable gauche and anti conformations. Of course, the torsions flanking the double bond (C18–C19 and C20–C21) are expected to cluster around skew and syn conformations instead, and they do, except that C20–C21 is a torsion that remains skew in all 21 structures. The torsions flanking the isolated keto group (C21–C22 and C22–C23) show a rather large spread of values, and do not appear to be easily categorized into gauche or anti conformations.

A major reason for the absence of the X-ray crystal structure from the set is the presence of intramolecular hydrogen bonds. The actual X-ray structure does not have any intramolecular hydrogen bonds, but one (O6—H1···O4) was formed upon energy minimization (Figure 4). This hydrogen bond is present in all the other structures; furthermore, 16 of these structures have additional hydrogen bonds involving O10–H2 as a donor (Table III). In the actual crystal structure, O10–H2 acts as an intermolecular hydrogen bond donor to O9 of a neighboring molecule.[7] In addition, one water molecule was located in the crystal which forms the hydrogen bonds O6—H1···O(W) and O(W)—H···O4, preventing the formation of a direct hydrogen bond between O6—H1 and O4. The water molecule also forms a hydrogen bond to O3 of a neighboring FK506 molecule. Another intriguing difference in the crystal structure is the anti orientation about the C25–C26 bond. The orientation is invariably gauche in the 21 other structures, which facilitates the intramolecular hydrogen bonding with O10–H2.

Table III. Intramolecular Hydrogen Bonds in the Structures Found in the Monte Carlo Search[a]

conformation	hydrogen bonds
1	O6···H1···O4; O10—H2···O8
2	O6—H1···O4; O10—H2···O5; O10—H2···O1
3	O6—H1···O4
4	O6—H1···O4; O10—H2···09
5	O6—H1···O4
6	O6—H1···O4; O10—H2···05; O10—H2···O1
7	O6—H1···O4; O10—H2···09
8	O6—H1···O4
9	O6—H1···O4; O10—H2···09
10	O6—H1···O4
11	O6—H1···O4; O10—H2···09
12	O6—H1···O4; O10—H2···08
13	O6—H1···O4; O10—H2···09
14	O6—H1···O4; O10—H2···03; O10—H2···O1
15	O6—H1···O4; O10—H2···01
16	O6—H1···O4; O10—H2···09
17	O6—H1···O4
18	O6—H1···O4; O10—H2···09
19	O6—H1···O4; O10—H2···09
20	O6—H1···O4; O10—H2···09
21	O6—H1···O4; O10—H2···05
X-ray (minimized)	O6—H1···O4

[a] A hydrogen bond is deemed to exist if the distance between the hydrogen and the acceptor is less than 2.5 Å and the donor–hydrogen–acceptor angle is greater than 120°.

Molecular Dynamics

Procedure. In order to investigate the dynamical behavior and solvation of FK506, a molecular dynamics (MD) simulation of the molecule in water was performed. The energy-minimized X-ray structure was taken as the starting point for the MD simulation. This structure was immersed in a box of TIP3P water molecules.[28] Any water molecule with its oxygen atom closer than 1.5 Å or with a hydrogen closer than 0.5 Å to any FK506 atom was removed. Any water molecule with its oxygen farther away than 7.0 Å from any solute atom in the *x*, *y*, or *z* directions was also removed, resulting in a system consisting of the solute

(28) Jorgensen, W. L.; Chandrasekhar, J.; Madura, J. D.; Impey, R. W.; Klein, M. L. *J. Chem. Phys.* **1983**, *79*, 926.

DOCKET ALARM

Explore Litigation Insights

Docket Alarm provides insights to develop a more informed litigation strategy and the peace of mind of knowing you're on top of things.

Real-Time Litigation Alerts

Keep your litigation team up-to-date with **real-time alerts** and advanced team management tools built for the enterprise, all while greatly reducing PACER spend.

Our comprehensive service means we can handle Federal, State, and Administrative courts across the country.

Advanced Docket Research

With over 230 million records, Docket Alarm's cloud-native docket research platform finds what other services can't. Coverage includes Federal, State, plus PTAB, TTAB, ITC and NLRB decisions, all in one place.

Identify arguments that have been successful in the past with full text, pinpoint searching. Link to case law cited within any court document via Fastcase.

Analytics At Your Fingertips

Learn what happened the last time a particular judge, opposing counsel or company faced cases similar to yours.

Advanced out-of-the-box PTAB and TTAB analytics are always at your fingertips.

API

Docket Alarm offers a powerful API (application programming interface) to developers that want to integrate case filings into their apps.

LAW FIRMS
Build custom dashboards for your attorneys and clients with live data direct from the court.

Automate many repetitive legal tasks like conflict checks, document management, and marketing.

FINANCIAL INSTITUTIONS
Litigation and bankruptcy checks for companies and debtors.

E-DISCOVERY AND LEGAL VENDORS
Sync your system to PACER to automate legal marketing.